Journal of Molecular Structure 1144 (2017) 389–395

Contents lists available at ScienceDirect

Journal of Molecular Structure

journal homepage: http://www.elsevier.com/locate/molstruc

Crystal structure, vibrational, spectral investigation, quantum chemical DFT calculations and thermal behavior of Diethyl [hydroxy (phenyl) methyl] phosphonate

Louiza Ouksel [a, *], Salah Chafaa [a], Riadh Bourzami [a], Noudjoud Hamdouni [b], Miloud Sebais [b], Nadjib Chafai [a]

[a] Laboratoire d'Electrochimie des Matériaux Moléculaires et des Complexes (LEMMC), Département de Génie des Procédés, Faculté de Technologie Université Ferhat Abbas, Sétif-1, 19000, Algeria
[b] Laboratoire de Crystallographie, Département de Physique, Faculté des Sciences Exactes, Université des Frères Mentouri Constantine-1, 25000, Algeria

ARTICLE INFO

Article history:
Received 14 February 2017
Received in revised form
27 April 2017
Accepted 10 May 2017
Available online 10 May 2017

Keywords:
Diethyl [hydroxy (phenyl) methyl] phosphonate
Crystal structure
FT-IR
FT-Raman
DFT calculation

ABSTRACT

Single Diethyl [hydroxy (phenyl) methyl] phosphonate (DHPMP) crystal with chemical formula $C_{11}H_{17}O_4P$, was synthesized via the base-catalyzed Pudovik reaction and Lewis acid as catalyst. The results of SXRD analyzes indicate that this compound crystallizes into a mono-clinic system with space group $P2_1/n$ symmetry and Z = 4. The crystal structure parameters are a = 9.293 Å, b = 8.103 Å, c = 17.542 Å, β = 95.329° and V = 1315.2 Å^3, the structure displays one inter-molecular O—H···O hydrogen bonding. The UV–Visible absorption spectrum shows that the crystal exhibits a good optical transmission in the visible domain, and strong absorption in middle ultraviolet one. The vibrational frequencies of various functional groups present in DHPMP crystal have been deduced from FT-IR and FT-Raman spectra and then compared with theoretical values performed with DFT (B3LYP) method using 6-31G (p, d) basis sets. Chemical and thermodynamic parameters such as: ionization potential (I), electron affinity (A), hardness (σ), softness (η), electronegativity (χ) and electrophilicity index (ω), are also calculated using the same theoretical method. The thermal decomposition behavior of DHPMP, studied by using thermogravimetric analysis (TDG), shows a thermal stability until to 125 °C.

1. Introduction

Organophosphorus compounds containing carbon-phosphorus (C–P) bonds have been attracting significant attention, ever since the first discovery in natural products in 1959 [1,2]. This compound family has found various applications in the pharmacology and agrochemical fields, medicinal chemistry [3–7] and biological activities as enzyme inhibitors [8], owing to their chemical stability and their noteworthy physicochemical properties [9–11]. At the present time, organophosphorus compounds include many subclasses such as phosphonates, α-aminophosphonates and α-hydroxyphosphonates. The last subclass compounds are used as precursors for a significant variety of phosphonates derivatives [12,13]. The α-hydroxyphosphonates can be synthesized according to several approaches. The most used approach is based on the reaction of aldehyde or ketone with dialkyl phosphite in the presence of acidic or basic catalysts, via the base-catalyzed Pudovik reaction [14]. These compounds are also synthesized via Michaelis-Arbuzov rearrangement reaction (transformation from trivalent to pentavalent phosphorus), in the presence of different catalysts [8,15–17]. Few synthesis routes of α-hydroxyphosphonates have been developed using Lewis acids as catalyst [18]. In this work, synthesis of Diethyl hydroxy (phenyl) methyl phosphonate (DHPMP) was reported using cobalt (II) chloride as Lewis acid catalyst. Cobalt (II) chloride is the adequate catalyst due to its extensive use in numerous reactions [19–23], its large availability and low price, it can also easily be removed from the reaction mixture [8].

Single crystal X-Ray Diffraction (SXRD) and quantum chemical calculation, were used in order to confirm the structure of DHPMP. The spectral study using FT-IR, FT-Raman and UV–visible analyses were also conducted in order to confirm whether a certain correlation exists between molecular structure and vibrational frequencies of DHPMP. Thermogravimetric analysis of DHPMP was

* Corresponding author.
E-mail address: louksel2014@gmail.com (L. Ouksel).

http://dx.doi.org/10.1016/j.molstruc.2017.05.029
0022-2860/

also performed.

2. Experimental procedures

2.1. Synthesis

The Diethyl [hydroxy (phenyl) methyl] phosphonate (DHPMP) compound was synthesized by chemical reaction at room temperature of benzaldehyde (1 mmol, purity 99%, Sigma Aldrich), triethyl phosphite (1 mmol, purity 99%, Sigma Aldrich) and $CoCl_2 \cdot 6H_2O$ (1 mmol, purity 98%, Sigma Aldrich) as a catalyst, under nitrogen reflux. A blue color appeared after 1 h time. The progress of the reaction was followed by thin layer chromatography TLC on silica gel (ethyl acetate/n-hexane 1:4); a single spot was observed after 16 h. For purification, chloroform (10 ml) was added to the reaction mixture and then filtered to separate the catalyst, and then evaporated under vacuum to eliminate chloroform. To be sure that all catalyst present was removed, the obtained product was separated in funnel, adding distilled water (2 × 100 ml) and dichloromethane (2 × 50 ml). The organic phase was dried with Na_2SO_4. The reaction scheme is shown in Fig. 1.

Anal. ^{1}H NMR for DHPMP Aromatic-H: 7.49–7.36 (m, 5H), OCH_2: 4.06 (m, 4H) CH_3: 1.27 (m, 6H), CH_2: 4.87 (s, 2H).

The synthesized compound was dissolved in n-hexane till the boiling point and then allowed to crystallize by solvent evaporation for three weeks [24], the photograph of the grown crystal is shown in Fig. 2.

2.2. Single crystal X-ray diffraction (SXRD)

Patterns SXRD were performed at room temperature, using Bruker X caliber diffractometer, equipped with MoKα anticathod and a graphite monochromator (λ = 0.7107 Å). The refinement was performed by the full-matrix least square method using the Crystal program [25]. Anisotropic thermal factors were determined for all non-hydrogen atoms. Unit cell refinement using all observed reflections and data reduction was performed using CrysAlis Red program. The structure was visualized by the Mercury software.

2.3. UV–Visible spectroscopy

After solubilizing DHPMP in ethyl acetate, UV–Visible spectrum was recorded with transmission mode at room temperature, in the range 200–800 nm, using a JASCO V680 spectrometer.

2.4. FT-IR spectroscopy

Spectra were recorded using a FT-IR 4200 JASCO spectrometer, in the range 4000–600 cm^{-1}, at room temperature.

2.5. Raman spectroscopy

Spectral measurements were made with a μ-Raman Bruker Senterra, equipped with a 100 mW laser source operated at

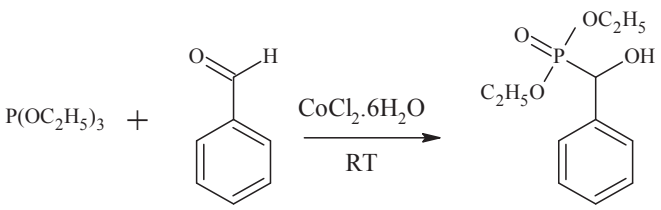

Fig. 1. Reaction scheme for synthesis of DHPMP.

Fig. 2. Photograph of DHPMP.

λ = 785 nm, and aperture setting about 20 × 1000 μm, the spectrum was situated in the range 3500 to 50 cm^{-1}.

2.6. Nuclear magnetic resonance ^{1}H NMR

Spectra were recorded at room temperature, on solution (solvent: DMSO-d_6), on a Bruker AV III 300 MHz spectrometer.

2.7. Thermal behavior analysis ATG-ATD

The thermogravimetric and differential thermal analysis were carried out using a Perkin Elmer TGA 4000 setup. The results were collected in the range of heating 5–600 °C, with a 5 °C/min speed, under a nitrogen atmosphere.

2.8. Quantum chemical calculations

The full geometry optimization was performed by means of the Gaussian 09 W program, based on density functional theory (DFT) [26], using Beck's three parameters hybrid functional exchange [27], with 6-31G (d. p) basis sets, and Lee-yang-Parr correlation functional (B3LYP) [28,29].

3. Results and discussion

3.1. SXRD analysis

Data collected by SXRD indicate that DHPMP crystal crystallizes in mono-clinic system with space group $P2_1/n$ and Z = 4. The crystal structure parameters are a = 9.293(5) Å, b = 8.103(5) Å, c = 17.542(5) Å, β = 95.329(5) °.The detailed fractional atomic coordinates and equivalent isotropic displacement parameters were deposited in CCDC with the reference number 1488904.

The DHPMP crystalline structure has been given by Li-Tao An and al. [30]. The present work extended furthermore the study by refining and detailing crystalline structure, where results were completed with DFT quantum chemical calculation. The experimental crystal data and structure refinement details are given in Table 1.

The asymmetric unit of DHPMP contains one formal molecule with the chemical formula $C_{11}H_{17}O_4P$ (Fig. 3).

The presence of C(6)–P(1) and C(6)–OH bonds confirms the formation of a hydroxy-phosphonate compound. The distances between the two carbons C(11)–C(16) and C(10)–C(15) are 1.260(1) Å and 1.407(9) Å respectively. These differences between

Table 1
Crystallographic data and structure refinement parameters.

Empirical formula	$C_{11}H_{17}0_4P$
Crystal system	Monoclinic
Space group	$P2_1/n$
a (Å)	9.293 (5)
b (Å)	8.103 (5)
c (Å)	17.542 (5)
β (°)	95.329 (5)
Temperature (K)	293
V (Å^3)	1315.2 (4)
Z	4
molecular weight (g/mol)	244.23
λMoKα (Å)	0.71073
D_{calc} (mg/m^3)	1.23
μ (mm^{-1})	0.21
F(000)	520
Crystal size (mm^3)	6 × 2 x 1
Crystal color/habit	White/Parallelepiped
θ Range (°)	3.342–32.352
hkl ranges	
h	−13 → 7
k	−12 → 9
l	−25 → 26
Measured reflections	8818
Independent reflections	4164
Observed reflections	1634
R_{int}	0.035
$(\sin\theta/\lambda)_{max}$ (Å^{-1})	0.753
Completeness to $2\theta = 26.20$	88.6%
Goodness-of-fit on F^2	0.8961
$R[F^2 > 2\sigma(F^2)]$	0.079
No. of reflections	1256
No. of parameters	146
$\Delta\rho_{max}$, $\Delta\rho_{min}$ (e Å^{-3})	0.28, −0.28

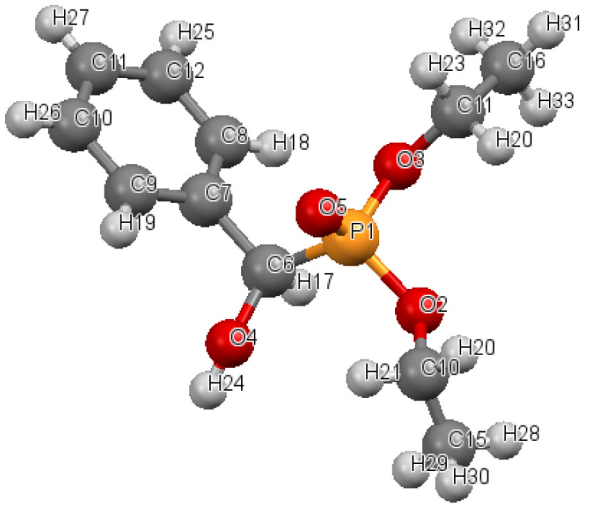

Fig. 3. Asymmetric unit.

the two values cause a deformation of the two ethyl groups of DHPMP. Benzene ring is distorted compared to ideal hexagonal shape so that the internal angles are (120.2 (7) °, 120.2 (6) °, 121.1 (5) °, 119.8 (7) °, 119.7(5) °, 119.1 (4) °). This difference is attributed to the lone pair electron steric effect, which is in good agreement with the theory of valence-shell electron pair repulsion (VSEPR) [31].

The unit cell structure of DHPMP is shown in Fig. 4, where the mono-clinic unit cell is centro-symmetric containing four molecules Z = 4. Table 2 lists the experimental geometrical parameters (length bonds and angle measurements) in comparison with

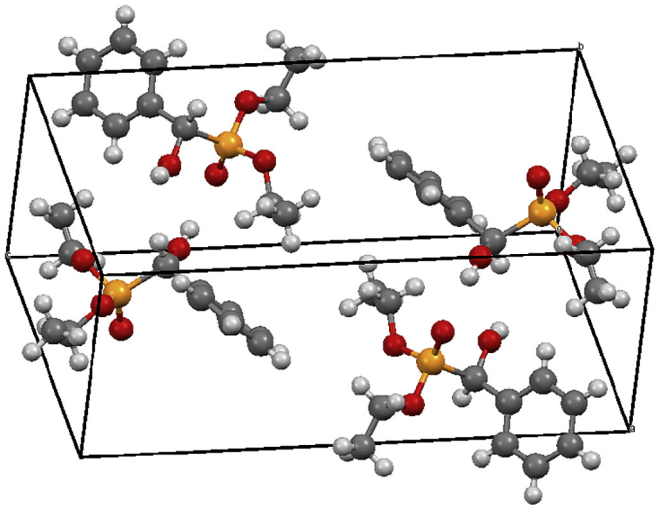

Fig. 4. Packing of the molecules in elementary unit cell.

quantum calculated values.

The hydrogen atoms are all located in a difference map, but those attached to the carbon atoms are repositioned geometrically. The hydrogen atoms were initially refined with soft restraints on the bond lengths and angles to regularize their geometry (C–H in the range 0.93–0.98 Å and O–H = 0.82 Å), after which the positions were refined with riding constraints [32]. The hydrogen bond O—H···O between the oxygen bonded with hydrogen as donor and the oxygen in double-bond with the phosphorus as acceptor developing thereby, three-dimensional chiral supra-molecular network [30]. This hydrogen bond deforms the C(6)-O(4)-H(24) angle, to form the crystalline structure (the experimental SXRD value is 144.6(5) ° and the calculated one is 109.4(6) °). Table 3 shows the proposed hydrogen bond with the corresponding acceptor-donor distances and its symmetry codes.

3.2. UV–Vis analysis

The optical absorption spectrum of DHPMP (Fig. 5) exhibits a strong absorption band around 258 nm (ε_{258} = 17626 L mol^{-1} cm^{-1}) assigned to the aromatic systems or electronic excitation in this region [33,34]. In general, the absorption band of benzene are mainly located around 200 nm related to the energy required for π-π* transition [34]. The absorption is negligible in visible range with a cut-off wavelength 292 nm, which is sufficient for laser frequency doubling and other related opto-electronic applications in ultra violet domain [35].

3.3. FT-IR/Raman analysis

The FT-IR spectrum of DHPMP crystal is shown in Fig. 6 (a). The characteristic vibration frequencies of the functional groups present in the title crystal were assigned and collected in Table 4. The broad band around 3626 cm^{-1} is due to symmetric stretching vibrations of O–H, while C–H aromatic and aliphatic stretching vibrations are observed at 3008 and 2925 cm^{-1} respectively. Sharp band observed at 1646 cm^{-1} is attributed to benzene ring stretching vibrations, whereas C–H deformation asymmetric mode of CH_3 and CH_2 occur at 1493 cm^{-1} and 1392 cm^{-1}. The medium IR band at 1362 cm^{-1} is assigned to O–H in plan bending mode of vibration. The band corresponding to P=O stretching mode of vibrations appears at 1231 cm^{-1}. The medium strong band at 698 cm^{-1} is due to symmetric ring mode vibrations, characteristic

Table 2
Calculated and experimental geometrical parameters (Å, °) of DHPMP.

Bond	Exp.	Calc.	Bond	Exp.	Calc.
P(1)–O(5)	1.464(3)	1.487(2)	C(16)–H(33)	0.960(4)	1.093(7)
P(1)–O(2)	1.571(3)	1.618(4)	C(6)–O(4)	1.425(5)	1.415(7)
P(1)–O(3)	1.577(4)	1.623(6)	C(7)–C(6)	1.520(6)	1.515(5)
P(1)–C(6)	1.819(4)	1.855(2)	C(6)–H(17)	1.008(4)	1.102(4)
O(2)–C(10)	1.398(6)	1.450(5)	O(4)–H(24)	0.822(3)	0.968(1)
C(11)–C(16)	1.407(9)	1.515(2)	C(16)–H(33)	0.960(4)	1.093(4)
C(11)–H(23)	0.982(8)	1.098(6)	C(10)–C(15)	1.370(7)	1.516(7)
C(10)–H(22)	0.970(7)	1.094(8)	C(7)–C(9)	1.384(7)	1.401(6)
C(15)–H(30)	0.970(6)	1.093(7)	C(12)–C(8)	1.400(1)	1.396(2)
O(3)–C(11)	1.440(9)	1.451(4)	C(8)–H(18)	0.944(3)	1.083(5)
C(11)–C(16)	1.260(1)	1.515(8)	C(12)–C(14)	1.370(1)	1.395(5)
C(11)–H(22)	0.970(8)	1.095(5)	C(12)–H(25)	0.935(6)	1.086(4)
C(11)–H(23)	0.954(7)	1.094(8)	C(14)–C(13)	1.360(1)	1.396(5)
C(16)–H(31)	0.961(6)	1.094(5)	C(14)–H(27)	0.949(6)	1.086(2)
C(16)–H(32)	0.920(5)	1.093(4)	C(9)–C(13)	1.381(9)	1.394(2)
C(9)–H(19)	0.940(7)	1.086(2)	C(13)–H(26)	0.938(8)	1.086(1)
C(10)–C(15)	1.407(9)	1.516(1)	C(4)–H(41)	0.982(8)	1.093(4)
C(15)–H(29)	0.953(6)	1.093(2)	C(15)–H(28)	0.965(5)	1.094(7)
C(7)–C(8)	1.399(8)				

Angles	Exp.	Calc.	Angles	Exp.	Calc.
O(5)–P(1)–O(2)	115.8(2)	115.1(6)	P(1)–O(3)–C(11)	121.9(4)	122.5(2)
O(5)–P(1)–O(3)	114.4(2)	11 3.9(7)	O(3)–C(11)–C(16)	115.0(8)	114.0(6)
O(5)–P(1)–C(6)	114.9(2)	114.9(6)	O(3)–C(11)–H(22)	108.0(7)	109.1(3)
O(2)–P(1)–O(3)	102.1(2)	102.6(1)	O(3)–C(11)–H(23)	108.5(6)	109.4(4)
O(2)–P(1)–C(6)	101.6(2)	103.8(7)	C(16)–C(11)–H(23)	110.5(4)	109.7(3)
O(3)–P(1)–C(6)	106.9(2)	106.7(8)	C(16)–C(11)–H(22)	107.1(5)	108.0(5)
P(1)–O(3)–C(4)	122.6(3)	121.3(3)	H(23)–C(11) –H(22)	107.4(7)	108.3(8)
O(2)–C(10)–C(15)	105.8(5)	108.6(2)	C(11)–C(16)–H(31)	109.7(6)	109.3(8)
O(2)–C(10)–H(21)	108.0(3)	109.7(1)	C(11)–C(16)–H(32)	109.0(4)	109.6(2)
O(2)–C(10)–H(20)	109.3(4)	108.8(6)	C(11)–C(16)–H(33)	109.2(3)	109.6(6)
C(15)–C(10)–H(20)	108.9(6)	109.1(9)	H(31)–C(16) –H(32)	110.0(5)	109.4(1)
C(15)–C(10)–H(21)	109.0(5)	109.4(6)	H(31)–C(16) –H(33)	109.0(6)	109.9(8)
H(20)–C(10) –H(21)	108.6(3)	109.8(6)	H(32)–C(16) –H(33)	110.0(7)	109.3(4)
C(10)–C(15)–H(30)	108.3(4)	109.6(3)	P(1)–C(6)–O(4)	104.7(3)	104.9(1)
C(10)–C(15)–H(28)	110.1(5)	109.3(5)	P(1)–C(6)–C(7)	112.2(3)	112.1(5)
C(10)–C(15)–H(29)	107.3(6)	109.7(1)	P(1)–C(6)–H(17)	106.8(4)	109.0(7)
H(30)–C(15) –H(28)	111.1(4)	109.4(1)	O(4)–C(6)–C(7)	113.2(3)	110.3(7)
H(30)–C(15) –H(33)	111.2(5)	109.5(2)	O(1)–C(6)–H(17)	110.2(6)	108.1(5)
H(28)–C(15) –H(29)	108.8(3)	109.4(1)	C(7)–C(6)–H(17)	109.4(4)	106.9(6)
C(6)–O(4)–H(24)	144.6(5)	109.4(6)	C(12)–C(14)–H(27)	119.8(6)	119.9(7)
C(6)–C(7)–C(8)	121.2(4)	120.4(4)	C(13)–C(14)–H(27)	120.0(5)	120.0(1)
C(6)–C(7)–C(9)	119.7(4)	119.3(2)	C(14)–C(13)–C(9)	119.8(7)	119.9(5)
C(8)–C(7)–C(9)	119.1(4)	120.2(1)	C(14)–C(13)–H(26)	120.7(4)	120.0(6)
C(7)–C(8)–C(12)	119.7(5)	119.8(2)	C(9)–C(13)–H(26)	119.5(3)	119.9(7)
C(7)–C(8)–H(18)	120.0(6)	120.0(4)	C(7)–C(9)–C(13)	121.1(5)	120.1(6)
C(12)–C(8)–H(18)	120.3(4)	120.1(3)	C(7)–C(9)–H(19)	118.2(6)	119.0(3)
C(8)–C(12)–C(14)	120.2(6)	119.9(3)	C(13)–C(9)–H(19)	120.7(3)	120.7(1)
C(8)–C(12)–H(25)	119.3(5)	119.8(2)	C(12)–C(14)–H(27)	119.8(6)	119.9(7)
C(14)–C(12)–H(25)	120.5(4)	120.0(1)	C(13)–C(14)–H(27)	120.0(5)	120.0(1)
C(12)–C(14)–C(13)	120.2(7)	120.0(1)	C(14)–C(13)–C(9)	119.8(7)	119.9(5)
C(16)–C(11)–H(22)	107.1(5)	109.6(5)	O(4)–C(6)–C(7)	113.2(3)	112.7(8)
O(4)–C(6)–H(17)	110.2(6)	109.8(1)	C(16)–C(11)–H(23)	110.5(4)	110.8(3)
C(16)–C(11)–H(22)	107.1(5)	108.3(2)			

Table 3
Hydrogen-bond geometry (Å, °).

D—H···*A*	*D*—H	H···*A*	*D*···*A*	*D*—H···*A*
O(4)–H(24)···O(5)[a]	0.822	2.701	2.701(9)	130.6(2)

[a] Symmetry code: (i) $-x+3/2, y-1/2, -z+1/2$.

of benzene monosubstituted.

Fig. 6 (b) shows FT-Raman spectrum of DHPMP with the

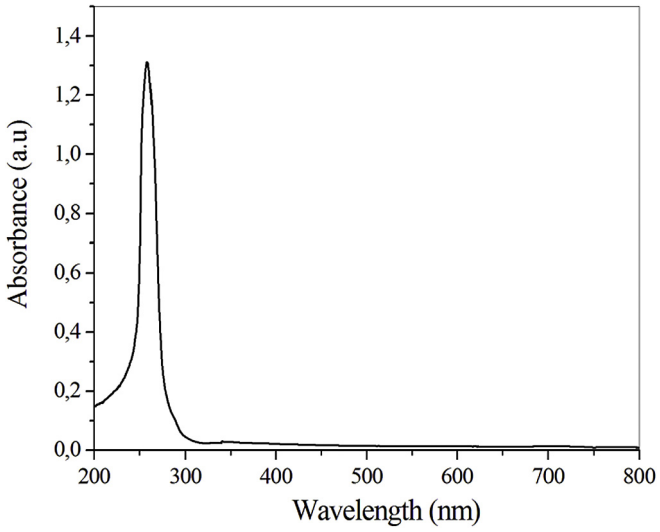

Fig. 5. UV–Vis absorption spectrum.

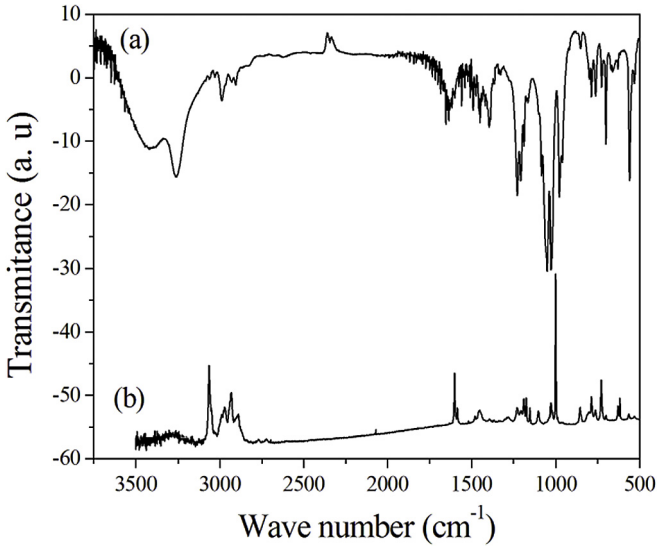

Fig. 6. (a) FT-IR spectrum, (b) Raman spectrum.

vibrational band assignments given in Table 4. The most intense band at 1002 cm^{-1} is due to symmetric vibrations of benzene ring. C–H stretching mode of vibration was observed at 3070 cm^{-1}. The weak band which appears at 1454 cm^{-1} is due to CH_2 bending mode. The band observed at 1216 cm^{-1} is assigned to P=O stretching vibration, and the medium bands at 1027 cm^{-1} and 725 cm^{-1} are attributed to P–O and P–C vibration modes respectively. The last three frequency values confirm the presence of phosphonate group in DHPMP structure. The symmetric stretching modes of C–O and C–C appear at 1172 cm^{-1} and 859 cm^{-1} respectively. The weak band at 775 cm^{-1} is due to ring-sextant out of plane deformation. Ring bending vibration occurs at 627 cm^{-1} in the case of benzene. All the corresponding calculated vibration bonds are shown in Table 4.

3.4. Quantum chemical calculations

3.4.1. Molecular electrostatic potential (MEP)

In this work and for molecular electrostatic potential and

Table 4
Experimental and theoretical vibration frequencies and assignments (the relative IR and Raman intensities normalized by highest peak absorption to 100).

Experimental frequencies (cm^{-1})		Calculated frequencies (cm^{-1})		Calculated Intensités		Assignments
IR	Raman	Unscaled	Scaled	IR	Raman	
3626	–	3709	3565.83	000.00	004.87	O–H asymmetric stretch of alcohol
3228	–	3217	3092.82	004.26	064.40	O–H symmetric stretch of alcohol
3008	3070	3119	2998.60	000.17	032.50	C–H aromatic stretch
2925	2935	3050	2932.27	000.03	100.00	C–H aliphatic asymmetric stretch
2875	2893	3034	2916.88	000.01	018.63	C–H aliphatic symmetric stretch
1646	1605	1659	1594.96	002.62	027.19	Benzene ring
1493	–	1504	1445.94	002.56	010.27	Ring stretch
1455	1454	1494	1436.33	003.76	026.44	CH_2 bending modes
1392	–	1419	1364.22	001.85	001.28	CH_3 bending
1231	1216	1307	1256.54	005.61	010.17	P=O stretching
_	1172	1294	1244.05	015.67	005.80	C–OH in alcohol, C–O stretch
_	1177	1197	1150.79	100.00	025.92	Rocking vibration for P–O–Et
_	1110	1179	1133.49	054.59	002.20	Benzene C–H deformation
_	1102	1165	1120.03	060.75	001.02	Benzene C–C deformation
1047	–	1156	1111.37	055.02	000.68	C–C symmetric stretching
_	1027	1056	1015.23	047.27	007.00	P–O symmetric stretching
_	1002	1012	0972.93	001.56	009.03	Ring breath and Benzene C=C
_	859	886	0851.80	016.32	000.20	C–C stretch
_	775	841	0808.53	016.49	001.10	Ring-sextant out-plane deformation
_	725	778	0747.96	008.49	000.62	P–C stretching
698	–	706	0678.74	000.58	000.98	Benzene monosubstituted
_	627	634	0609.52	002.66	003.47	Ring bend
604	617	625	0600.87	053.53	000.97	Benzene ring: quadrant out-of-Plane
_	–	399	0383.59	000.37	000.18	O–H asymmetric stretch of alcohol
_	–	238	0228.81	000.51	002.15	Lattice vibration
_	–	99	0095.17	001.15	000.71	Lattice vibration

frontier orbital molecular calculations, a model of two molecules bonded by hydrogen bond was chosen, as shown in Fig. 7. This model approaches the crystalline structure of DHPMP.

The molecular electrostatic potential surface was determined by DFT calculations. For organophosphorus compounds, the total electron density surface mapped with electrostatic potential indicates the presence of a high negative charge on phosphorus and oxygen atoms [36,37]. The total electron density mapped with electrostatic potential surface of DHPMP and the electrostatic potential contour map for negative and positive potentials are shown in Fig. 7. The negative charge is indicated by red color, the blue region indicates the partially positive charge, the light blue region shows electron deficiency, the yellow region reveals the slightly rich electron and the green region shows neutral. The electrostatic potential of DHPMP is in the range - 10.710^{-2} V to + 10.710^{-2} V.

3.5. Frontier molecular orbitals (FMO_S)

The electron donor distribution in the highest occupied molecular orbital (HOMO) and the electron acceptor distribution in the lowest unoccupied molecular orbital (LUMO) are calculate and the result is shown in Fig. 8. The calculated energies values of HOMO

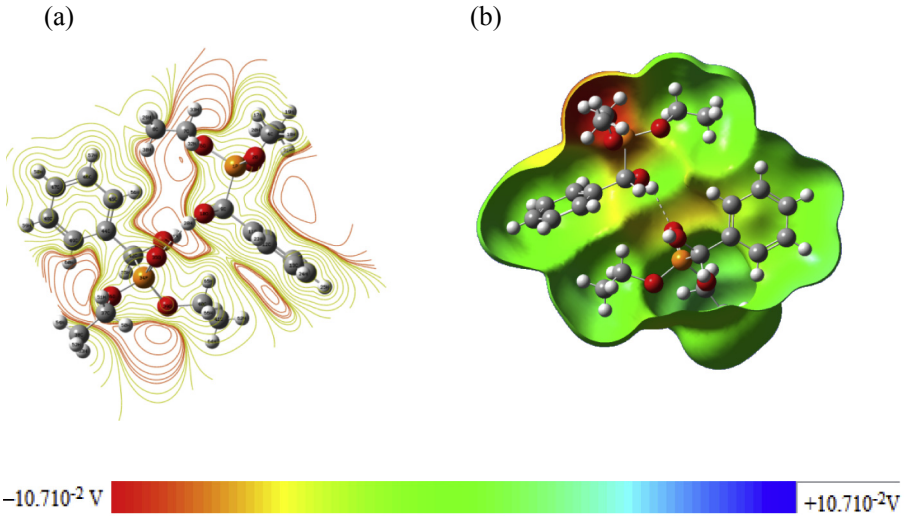

Fig. 7. (a) The contour map of electrostatic potential (b) The total electron density mapped with electrostatic potential.

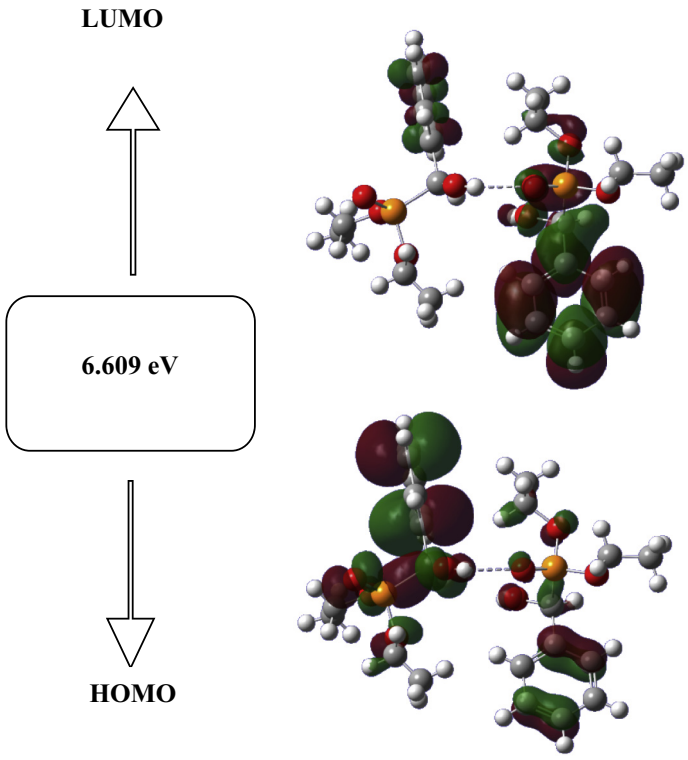

Fig. 8. Molecular orbitals.

Table 5
Calculated quantum chemical and thermodynamic parameters.

Quantum chemical parameters	
Etot (eV)	−29163.27
E_{HOMO} (eV)	−6.785
E_{LUMO} (eV)	−0.175
Egap (Δ)	6.609
Ionization potentiel (I)	6.785
Electron affinity (A)	0.175
Global hardness (η)	3.304
Global softness (σ)	0.302
Electronegativity (χ)	3.480
Global electrophilicity (ω)	1.833
Chemical potentiel (μ)	−0.072
Thermodynamic parameters	
SCF energy (a. u.)	−2141.41
Total energy (thermal)	
Total	328.802
Electronic	0.0000
Translational	0.889
Rotational	0.889
Vibrational	327.025
Heat capacity at const volume (cal.mol^{-1}.K^{-1})	
Total	99.56
Electronic	0.0000
Translational	2.981
Rotational	2.981
Vibrational	93.598
Entropy (cal. mol^{-1}.K^{-1})	
Total	159.291
Electronic	0.0000
Translational	44.444
Rotational	36.658
Vibrational	78.189
Zero-point vibrational energy E_0 (Kcal. mol^{-1})	313.99
Rotational constants (GHz)	
X	0.18486
Y	0.10176
Z	0.07627

$I = -E_{HOMO}$, $A = -E_{LUMO}$, $\chi = -[1/2(E_{LUMO} + E_{HOMO})]$, $\eta = 1/2(E_{LUMO} - E_{HOMO})$, $\omega = \chi^2/2\eta$. $\sigma = 1/\eta$, $\mu = -1/[2(I + A)]$.

and LUMO were −6.785 eV and −0.175 eV respectively. The difference between them was the energy gap is found to be 6.609 eV.

Table 5 shows some calculated chemical properties of DHPMP such as: energies values of HOMO, LUMO levels and the gap, ionization potential (I), electron affinity (A), Global hardness (η), Global softness (σ), electronegativity (χ), Global electrophilicity (ω), Chemical potentiel (μ), and thermodynamic parameters. The results obtained for DHPMP are comparable to those found in the literature for organophosphorus compounds [36–38].

3.6. Thermal analysis

The TGA and DTA curves of DHPMP are shown in Fig. 9. First the

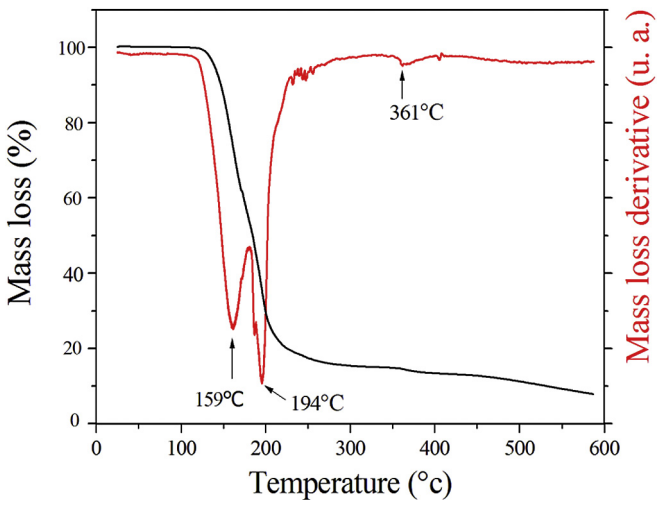

Fig. 9. TGA-DTA thermograms of DHPMP.

DHPMP crystals exhibit a thermal stability until to 125 °C; no mass loss observed around 100 °C, which indicates the absence of water molecule, which is due to water evaporation. Then, three stages weight loss process is observed: the first stage takes place in the temperature range of 125–172 °C, with DTA peak at 159 °C. These results are probably due to a break of the alkoxy group (O–C_2H_5) chemical bond [39]. The second stage is situated at the temperature range 172–210 °C with the corresponding TDA peak at 194 °C, which is assigned to P–C–$C_{armotic}$ decomposition. The two stages are characterized by a significant weight loss about 80%. The third stage takes place in the temperature range of 210–600 °C with the corresponding DTA peak at 361 °C this behavior could be assigned to phosphorus elimination [40].

4. Conclusion

Diethyl [hydroxy (phenyl) methyl] phosphonate (DHPMP) single crystal was synthesized and grown by slow solvent evaporation technique, its molecular formula was confirmed using single crystal X-ray diffraction to be $C_{11}H_{17}O_4P$, The mono-clinic unit cell is centro-symmetric with space group $P2_1/n$, containing four molecules $Z = 4$. The geometric parameters calculated by DFT confirmed the title crystalline structure. Theoretically predicted IR and Raman frequencies compared with experimental values were well assigned for the grown crystal, the obtained results are in good agreement with those found in the literature. It is to be noted that DHPMP possesses hydrogen bonds, those hydrogen bonds, responsible of the crystal chirality. These structural properties offer to the compound the possibility to deviate the polarized light. The spectrum shows that the absorption is negligible within the visible domain, with a 292 nm cut off wavelength. The latter value is sufficient for laser frequency doubling and other related opto-electronic applications in ultra violet domain. Another advantage for DHPMP crystal is its thermal stability, achieving experimentally up to 125 °C.

References

[1] H. Ait Youcef, S. Chafaa, R. Doufnoune, T. Douadi, J. Mol. Struct. 1123 (2016) 138–143.
[2] Z. Karimi-Jabiri, H. Zare, M. Amiri, N. Sadeghi, Chin. Chem. Lett. 22 (2011) 559–562.
[3] M. Juribasic, L. Tasek-Bosic, J. Mol. Struct. 924–926 (2009) 66–72.
[4] K.A. Schug, W. Lindner, Chem. Rev. 105 (2005) 67–114.
[5] K. Moonen, I. Lauryn, C.V. Stevens, Chem. Rev. 104 (2005) 6177–6215.
[6] R.L. Hildebrand, T.O. Henderson, In the Role of Phosphonate in Living Systems, CRC press, Boca Raton, 1983.
[7] S.R. Mandadapu, M.R. Gunnam, A.C.G. Kankanamalage, R.A.Z. Uy, K.R. Alliston, G.H. Lushington, Y. Kim, K-Ok Chang, W.C. Groutas, Bioorg. Med. Chem. Lett. 23 (2013) 5941–5944.
[8] G.S. Prasad, M. Manjunath, K.R.K.K. Reddy, O.V.S. Reddy, C.S. Reddy, Arkivoc (2006) 128–135.
[9] K.D. Karlin, Progress in Inorganic Chemistry, vol. 47, 1998, pp. 371–510. New York.
[10] K. Maeda, Micro. Meso. Mater. 73 (2004) 47–55.
[11] J.G. Mao, Coord. Chem. Rev. 251 (2007) 1493–1506.
[12] Q. Li, C.J. Hou, Y.J. Liu, R.F. Yang, X.P. Hu, Tetrahedron Asymmetry 26 (2015) 617–622.
[13] N.Z. Kiss, A. Kaszás, L. Drahos, Z. Mucsi, G. Keglevich, Tetrahedron Lett. 53 (2012) 207–209.
[14] L. Nagarapu, R. Mallepalli, U.N. Kumar, P. Venkateswarlu, R. Bantu, L. Yeramanchi, Tetrahedron Lett. 53 (2012) 1699–1700.
[15] V.K. Yadav, Synth. Commun. 20 (1990) 239–246.
[16] E.V. Mataveeva, I.L. Odinets, V.A. Kazlov, A.S. Shaplov, T.A. Mastryukova, Tetrahedron Lett. 47 (2006) 7645–7648.
[17] P.Y. Renard, P. Varon, E. Leclerc, A. Vallex, C. Mioskowski, Chem. Int. Ed. 42 (2003) 2389–2392.
[18] Ye-Q. Wen, R. Hertzberg, C. Moberg, J. Orga. Chem. 79 (2014) 6172–6178.
[19] S.K. De, Heteroat. Chem. 19 (2008) 592–595.
[20] S.K. De, Tetrahedron Lett. 45 (2004) 1035–1036.
[21] F. Fringuelli, F. Pizzo, L. Vaccaro, Synthesis 5 (2000) 646–650.
[22] R.R. Srivastava, G.W. Kabalka, Tetrahedron Lett. 33 (1992) 593–594.
[23] A.A. Dabbawala, D.U. Parmar, H.C. Bajaj, R.V. Jasra, J. Mol. Catal. A Chem. 282 (2008) 99–106.
[24] B. Kaboudin, Tetrahydron Lett. 41 (2000) 3169–3171.
[25] P.W. Betteridge, J.R. Carruthers, R.I. Cooper, K. Prout, D.J. Watkin, J. Appl. Cryst. 36 (2003), 1487–1487.
[26] W. Kohn, L.J. Sham, Phys. Rev. 140 (1965) 1133–1138.
[27] A.D. Becke, J. Chem. Phys. 98 (1993) 5648–5652.
[28] C. Lee, W. Yang, R.G. Parr, Phys. Rev. 37 (1998) 785–789.
[29] B. Miehlich, A. Savin, A. Stoll, H. Preuss, Chem. Phys. Lett. 157 (1989) 200–206.
[30] L.T. An, G.X. Gong, X. Liu, M. Xia, J.F. Zhou, Acta Crist. E 64 (2008) 1320–1327.
[31] R.P. Gillespie, J. Chem. Educ. 40 (1963) 295–301.
[32] R.I. Cooper, A.L. Thompson, D.J. Watkin, J. Appl. Cryst. 43 (2010) 1100–1107.
[33] K. Kirubavathi, K. Selvaraju, S. Kumararaman, Spectrochim. Acta A 71 (2008) 1–4.
[34] G. Madhurambal, B. Ravindran, M. Mariappan, S.C. Mojumdar, J. Therm. Anal. Calorim. 100 (2010) 811–815.
[35] Y. Le Fur, R. Masse, M.Z. Cherkaoui, J.F. Nicoud, Z. Krist. 210 (1995) 856–860.
[36] A. Hellal, S. Chafaa, N. Chafai, J. Mol. Struct. 1103 (2017) 110–124.
[37] N. Chafai, S. Chafaa, K. Benbouguerra, D. Daoud, A. Hellal, M. Mehri, J. Taiwan Inst. Chem. Eng. 70 (2016) 331–344.
[38] V. Arjunan, M. Kalaivani, M.K. Marchewka, S. Mohan, J. Mol. Struct. 1045 (2013) 160–170.
[39] M.A. De Souza Rios, S.E. Mazzetto, Fuel Process. Technol. 96 (2012) 1–8.
[40] A.I. Balabanovich, V.P. Prokopovich, J. Anal. Appl. Pyrolysis 76 (2006) 169–177.